Detection of a C4a-Hydroperoxyflavin Intermediate in the Reaction of a Flavoprotein Oxidase[†]

Jeerus Sucharitakul,[‡] Methinee Prongjit,[§] Dietmar Haltrich,[||] and Pimchai Chaiyen*[,§]

Department of Biochemistry, Faculty of Dentistry, Chulalongkorn University, Henri-Dunant Road, Patumwan, Bangkok 10300, Thailand, Department of Biochemistry and Center for Excellence in Protein Structure and Function, Faculty of Science, Mahidol University, Bangkok 10400, Thailand, and Department of Food Science and Technology, BOKU-University of Natural Sources and Applied Life Sciences, Vienna A-1190, Austria

Received June 5, 2008; Revised Manuscript Received July 7, 2008

ABSTRACT: This work describes for the first time the identification of a reaction intermediate, C4a-hydroperoxyflavin, during the oxidative half-reaction of a flavoprotein oxidase, pyranose 2-oxidase (P2O) from *Trametes multicolor*, by using rapid kinetics. The reduced P2O reacted with oxygen with a forward rate constant of 5.8×10^4 M^{-1} s^{-1} and a reverse rate constant of 2 s^{-1}, resulting in the formation of a C4a-hydroperoxyflavin intermediate which decayed with a rate constant of 18 s^{-1}. The absorption spectrum of the intermediate resembled the spectra of flavin-dependent monooxygenases. A hydrophobic cavity formed at the *re* side of the flavin ring in the closed state structure of P2O may help in stabilizing the intermediate.

Flavin-dependent oxidases contain flavin adenine dinucleotide (FAD)[1] or flavin mononucleotide (FMN) as a cofactor for the oxidation of a wide variety of substrates, including amino acids, carbohydrates, amines, fatty acids, alcohols, and others (*1–3*). The overall reaction can be divided into a reductive and an oxidative half-reaction. In the reductive half-reaction, the flavin cofactor is reduced concomitantly with the oxidation of an electron donor substrate. In the following oxidative half-reaction, the cofactor is reoxidized concurrently with the reduction of molecular oxygen, which is converted to H_2O_2. This latter half-reaction involves the chemistry of reduced flavin and dioxygen, one of the most fascinating and complex subjects in enzymology that has been investigated extensively over the past few decades (*4–7*).

The first step of the reaction of reduced flavin and oxygen is believed to involve a one-electron transfer from the reduced flavin to dioxygen to form a radical pair of a neutral flavin semiquinone and a superoxide, $FlH^{\bullet}\cdot O_2^{\bullet-}$ (Figure 1, step 1) (*2, 4, 5*). In the flavin-dependent monooxygenase reaction, the radical pair collapses into a flavin C4a-peroxide, which is then protonated to yield a C4a-hydroperoxyflavin

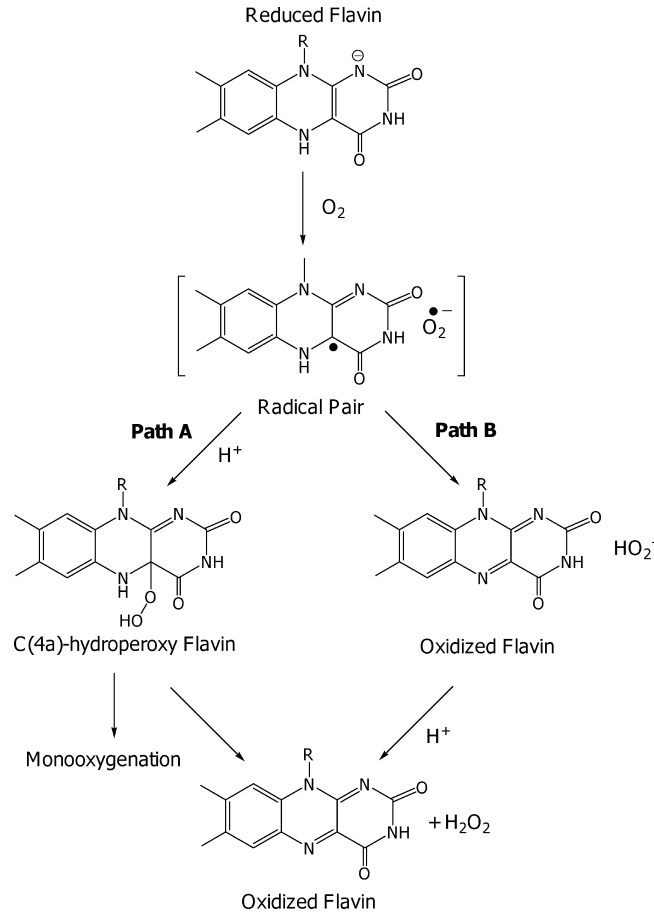

FIGURE 1: Reaction of reduced flavin and oxygen in flavoprotein monooxygenases (path A) and oxidases (path B).

[†] This work was supported by the The Thailand Research Fund through Grant BRG5180002 to P.C. and Grant MRG4980117 to J.S. and Royal Golden Jubilee Ph.D. Program Grant PHD/0151/2547 to M.P. Grants from the Faculty of Science of Mahidol University to P.C. and Dental Research Fund from the Faculty of Dentistry of Chulalongkorn University to J.S. are also acknowledged. D.H. was supported by a grant from the Austrian Research Foundation (FWF Translational Project L213-B11).

* To whom correspondence should be addressed: Department of Biochemistry and Center for Excellence in Protein Structure and Function, Faculty of Science, Mahidol University, Rama 6 Road, Bangkok 10400, Thailand. Telephone: 662-2015596. Fax: 662-3547174. E-mail: scpcy@mucc.mahidol.ac.th.

[‡] Chulalongkorn University.

[§] Mahidol University.

[||] BOKU-University of Natural Sources and Applied Life Sciences.

[1] Abbreviations: P2O, pyranose oxidase; GO, glucose oxidase; ChO, choline oxidase; C_2, oxygenase component of *p*-hydroxyphenylacetate hydroxylase; FAD, flavin adenine dinucleotide; FMN, flavin mononucleotide; Fl_{red}, reduced FAD; Fl_{ox}, oxidized FAD; Fl-OOH, C4a-hydroperoxy-FAD; AldOx, alditol oxidase; k_{app}, apparent rate constant.

10.1021/bi801039d CCC: $40.75
Published on Web 07/25/2008

intermediate that is able to eliminate H_2O_2 rapidly in the absence of monooxygenating targets (Figure 1, path A). Stopped-flow studies have shown that the C4a-hydroperoxyflavin or C4a-peroxyflavin is a common intermediate in the reactions of flavin-dependent monooxygenases. The C4a-hydroperoxyflavin usually acts as an electrophile, while the C4a-peroxyflavin performs a nucleophilic attack in the monooxygenation reaction (*1, 5, 8*). Only in the C42S mutant of NADH oxidase, a member of the glutathione reductase class of pyridine nucleotide-dependent flavoprotein disulfide reductases, was the C4a-hydroperoxyflavin intermediate found outside the reaction of flavin-dependent monooxygenase (*9*). For flavin-dependent oxidases described above, however, attempts to detect intermediates in the oxidative half-reaction have failed, thus rendering the detailed reaction pathway subsequent to the formation of the radical pair an unanswered question and a matter of debate (*1, 2, 10*).

The formation of a C4a-hydroperoxyflavin intermediate has been considered a possible pathway for flavoprotein oxidases since the intermediate can eliminate H_2O_2 (Figure 1, path A). In the case of glucose oxidase (GO) from *Aspergillus niger*, the generation of a flavin semiquinone−superoxide radical pair using pulse radiolysis suggested the presence of a putative C4a-hydroperoxyflavin intermediate (*11*). However, the observed intermediate decayed to the oxidized enzyme at a rate of 350 s^{-1}, a rate which should make it possible to detect the intermediate by stopped-flow techniques. The failure to do so implies either that the rate of decay of the natural C4a-hydroperoxy-flavin is considerably more rapid than that of the intermediate generated by radiolysis or that the observed intermediate is an experimental artifact and not part of the authentic reaction mechanism (*1*).

Alternatively, after the flavin semiquinone−superoxide radical pair is formed, a second, direct one-electron transfer can take place, giving the same product outcome as in path A but without formation of a flavin intermediate (Figure 1, path B). Since there is no need for the flavin to perform nucleophilic or electrophilic attack as in the case of flavin-dependent monooxygenases, the stabilization of C4a-hydroperoxyflavin in flavoprotein oxidases is not a functional requirement. The architecture of the active sites in several flavoprotein oxidases would support the direct formation of H_2O_2 since the formation of C4a-hydroperoxyflavin is disfavored due to spatial constraints (*2, 12, 13*). However, the generality of this hypothesis is contradicted by the recently determined crystal structure of *Arthrobacter globiformis* choline oxidase (ChO) with a flavin C4a-adduct of unknown identity (PDB entry 2JBV) (*14*), showing that a flavin C4a-adduct can indeed be accommodated chemically, structurally, and spatially through a major conformational change in the flavin pyrimidine ring as a result of sp^3 hybridization at the C4a position. Therefore, the existence of a C4a-hydroperoxyflavin along the reaction coordinate of flavoprotein oxidases remains an open question.

Pyranose 2-oxidase (P2O, pyranose:oxygen 2-oxidoreductase, glucose 2-oxidase, EC 1.1.3.10) from *Trametes multicolor* is a 270 kDa homotetrameric flavoprotein oxidase, in which each subunit carries an 8α-(*N*3)-histidyl-linked FAD molecule, i.e., covalent attachment of the FAD C8 M atom to His167 $N^{\varepsilon 2}$ (*15*). The enzyme catalyzes the oxidation of D-glucose and other aldopyranoses at the C2 position, yielding 2-ketoaldose and H_2O_2 as products (*16*). It has previously been suggested that the closed, acetate-bound, state of P2O (*17*) provides a solvent-shielded environment for oxygen reactions and is a structural mimic for the active site during the oxidative half-reaction, whereas the complex of P2O with 2-fluoro-2-deoxy-D-glucose (2FG) (*18*) is compatible with only the active site during the reductive half-reaction.

Scheme 1

$$\text{E-Fl}_{red} + O_2 \underset{k_1 = 2\ s^{-1}}{\overset{k_1 = 5.8 \times 10^4\ M^{-1}s^{-1}}{\rightleftharpoons}} \text{E-Fl-OOH} \xrightarrow{k_2 = 18\ s^{-1}} \text{E-Fl}_{ox} + H_2O_2$$

Using transient-kinetics studies of P2O, we present here the first unambiguous direct evidence of a C4a-hydroperoxyflavin intermediate in the oxidative half-reaction of a flavoprotein oxidase. In the closed state of P2O, an elongated, mainly hydrophobic cavity was located at the *re* side of the flavin ring and may account for stabilization of the intermediate. This finding implies that P2O may represent a missing link in enzyme evolution and that monooxygenases capable of performing sophisticated oxygenation chemistry might have evolved from rather simpler oxidases.

EXPERIMENTAL PROCEDURES

Determination of P2O Molar Absorptivity. A solution of wild-type P2O was added to 6 M guanidinium hydrochloride (pH 7.0) to denature the enzyme (*19*). The flavin concentration of the denatured enzyme solution was calculated on the basis of the solution absorbance at 450 nm using an ε_{450} of 11.3 × 10^3 M^{-1} cm^{-1}, the known value for free FAD (*19*). The molar absorptivity of wild-type P2O at 458 nm (ε_{458}) was calculated, on the basis of the flavin content, to be 11.3 × 10^3 M^{-1} cm^{-1}, and this value was used throughout for preparation of P2O solutions.

Rapid-Kinetics Experiments. Unless otherwise specified, reactions were carried out in 50 mM sodium phosphate buffer (pH 7.0) at 4 °C. Rapid-kinetics measurements were performed using a stopped-flow spectrophotometer (Hi-Tech Scientific model SF-62DX) in single-mixing mode with an optical path length of the observation cell of 1 cm. The stopped-flow apparatus was made anaerobic by flushing the flow system with an anaerobic buffer solution containing protocatechuate/protochatechuate dioxygenase as described previously (*20*). The reduced enzyme was prepared in a glass tonometer and was stoichiometrically reduced with a solution of 10 mM D-glucose in 50 mM sodium phosphate buffer (pH 7.0) delivered from a syringe attached to the tonometer. The reduced enzyme solution was loaded onto the stopped-flow machine, and the reaction was monitored at various wavelengths. Apparent rate constants (k_{app}) from kinetic traces were calculated from exponential fits using *KinetAsyst3* (Hi-Tech Scientific, Salisbury, U.K.) or *Program A* (developed by R. Chang, C-J. Chiu, J. Dinverno, and D. P. Ballou, The University of Michigan, Ann Arbor, MI). Determinations of rate constants by a graphical method were performed on the basis of plots of k_{app} versus oxygen concentration using a Marquardt−Levenberg nonlinear fit algorithm implemented in *KaleidaGraph* (Synergy Software, Reading, PA). Simulations were performed by numerical methods using the Runge−Kutta algorithm implemented in Berkeley Madonna

8.3 with a time step of 10^{-3} s. A model of a two-step reversible reaction provided in the program was used.

Analysis of Kinetic Parameters. The sum and product of the two apparent rate constants of a two-step model can be described by eqs 1 and 2 (*21, 22*).

$$A \underset{k_{-1}}{\overset{k_{-1}}{\rightleftharpoons}} B \underset{k_{-2}}{\overset{k_{-2}}{\rightleftharpoons}} D$$

$$k_{app1} + k_{app2} = k_1 + k_{-1} + k_2 + k_{-2} \quad (1)$$

$$k_{app1}k_{app2} = k_1(k_2 + k_{-2}) + k_{-1}k_{-2} \quad (2)$$

Specify

$$k_{app1} + k_{app2} = A \quad (3)$$

$$k_{app1}k_{app2} = B \quad (4)$$

Substitute $k_{app1} = A - k_{app2}$ into eq 4 to obtain

$$-{k_{app2}}^2 + k_{app2}A - B = 0$$

$$k_{app2} = \frac{A \pm \sqrt{A^2 - 4B}}{2} = \frac{A}{2} \pm \frac{A}{2}\sqrt{1 - \frac{4B}{A^2}};$$

$$\sqrt{1 - \frac{4B}{A^2}} \approx 1 - \frac{2B}{A^2} \text{ when } A > B$$

Therefore, $k_{app2} = A - B/A$ or B/A and $k_{app1} = A - B/A$ or B/A

Since $k_{app1} > k_{app2}$

$$k_{app1} = A - B/A;\ k_{app1} = k_1 + k_{-1} + k_2 + k_{-2} - \frac{k_1k_2 + k_1k_{-2} + k_{-1}k_{-2}}{k_1 + k_{-1} + k_2 + k_{-2}} \quad (5)$$

$$k_{app2} = B/A;\ k_{app2} = \frac{k_1k_2 + k_1k_{-2} + k_{-1}k_{-2}}{k_1 + k_{-1} + k_2 + k_{-2}} \quad (6)$$

In the P2O reaction, the first step is a bimolecular reaction under a pseudo-first-order condition (Scheme 1); k_1 is thus substituted with $k_1[O_2]$. Since from simulations $k_{-2} = 0$, k_{app1} and k_{app2} of the oxidative half-reaction of P2O can be described by eqs 7 and 8.

$$k_{app1} = k_1[O_2] + k_{-1} + k_2 - \frac{k_1[O_2]k_2}{k_1[O_2] + k_{-1} + k_2} \quad (7)$$

$$k_{app2} = \frac{k_1[O_2]k_2}{k_1[O_2] + k_{-1} + k_2} \quad (8)$$

RESULTS

Kinetics of the Oxidative Half-Reaction of P2O. A solution of reduced P2O was mixed with buffers containing various oxygen concentrations using a stopped-flow spectrophotometer. The reactions were monitored at 458 nm and at various wavelengths in the 320−400 nm region. Traces at 395 nm indicate biphasic kinetics with an absorbance increase during the first phase and a decrease during the second phase (Figure 2A). Apparent rate constants of the first phase are linearly dependent on oxygen concentration (inset of Figure 2A). The slope of the plot indicates a bimolecular rate constant of 4.3 ± 0.4) × 10^4 M^{-1} s^{-1} and an intercept value of 18 s^{-1} (inset of Figure 2A). The decrease in absorbance at 395 nm in the second phase was concurrent with an increase in absorbance at 458 nm, indicating that the oxidized enzyme was formed during this phase (Figure 2A,B). Apparent rate constants of the second phase are hyperbolically dependent on oxygen concentration (inset of Figure 2B), approaching a value of 21 ± 2 s^{-1}. Traces of the wavelengths at 320−400 nm exhibited kinetics similar to the trace at 395 nm (data not shown). These data are consistent with a model in which

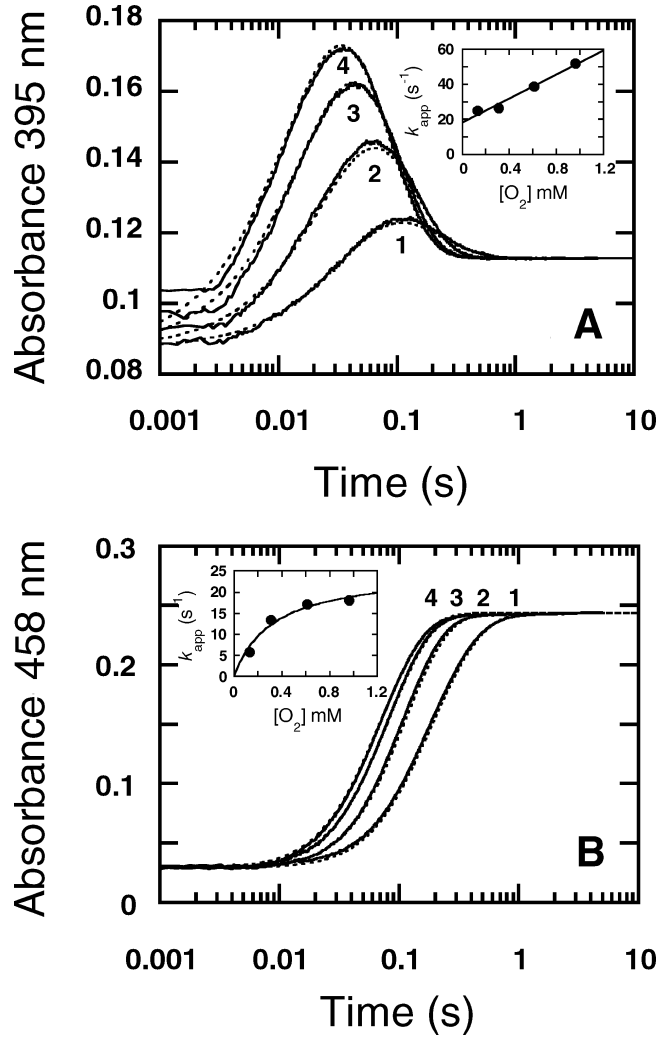

FIGURE 2: Reaction of reduced P2O with oxygen. A solution of the reduced enzyme (23 μM) was mixed with buffers containing various concentrations of oxygen [0.130 (1), 0.31 (2), 0.61 (3), and 0.96 mM (4)]. The reactions were performed in sodium phosphate buffer (pH 7.0) at 4 °C in a stopped-flow spectrophotometer, and all concentrations shown are final concentrations after mixing. [The highest oxygen concentration (1.9 mM before mixing) was achieved by bubbling the buffer syringe with 100% oxygen gas on ice.] The absorbances of the reactions were monitored at 395 (A) and 458 nm (B). The results indicate biphasic kinetics with an intermediate formed during the first phase (absorbance increase at 395 nm) and decayed during the second phase (absorbance decrease at 395 nm and increase at 458 nm). The second phase also coincided with the flavin oxidation, as shown by a large increase in absorbance at 458 nm. The inset in panel A shows a plot of apparent rate constants (k_{app}) of the first phase vs oxygen concentration. The inset in panel B shows a plot of the apparent rate constant (k_{app}) of the second phase vs oxygen concentration. Dotted lines represent simulations using the model in Scheme 1 and the following parameters: k_1 = 5.8 × 10^4 M^{-1} s^{-1}, k_{-1} = 2 s^{-1}, k_2 = 18 s^{-1}, ε_{395} of E−Fl_{red} = 4100 M^{-1} cm^{-1}, ε_{395} of E−Fl−OOH = 10300 M^{-1} cm^{-1}, ε_{395} of E−Fl_{ox} = 5210 M^{-1} cm^{-1}, ε_{458} of E−Fl_{red} = 1980 M^{-1} cm^{-1}, ε_{458} of E−Fl−OOH = 2000 M^{-1} cm^{-1}, and ε_{458} of E−Fl_{ox} = 11330 M^{-1} cm^{-1}.

Table 1: Comparison of Apparent Rate Constants (k_{app}) Obtained from Exponential Fits and Simulations

[oxygen] (μM)	k_{app} of the first phase[a] (s^{-1})	k_{app} of the first phase[b] (s^{-1})	k_{app} of the second phase[a] (s^{-1})	k_{app} of the second phase[b] (s^{-1})
130	24.7	22.6	6.0	4.9
310	30.0	29.5	11.6	8.5
610	45.0	43.6	14.6	11.4
960	58.0	62.7	16.0	13.3

[a] Apparent rate constants from exponential fits. [b] Apparent rate constants calculated from simulation parameters.

one intermediate with a λ_{max} of approximately 330−400 nm exists during the oxidative half-reaction of P2O.

The data were analyzed using kinetic simulations as described in Experimental Procedures. Simulations of the data using a model in Scheme 1 and kinetic parameters ($k_1 = 5.8 \times 10^4$ M^{-1} s^{-1}, $k_{-1} = 2$ s^{-1}, and $k_2 = 18$ s^{-1}) agree well with the experimental data (dashed versus solid lines in panels A and B of Figure 2). Calculations of apparent rate constants based on these numbers and the exact solution of a two-step consecutive reaction model (Experimental Procedures) were carried out to verify if the calculated and experimental values agreed. The results show that apparent rate constants calculated from simulation parameters using eqs 7 and 8 (Experimental Procedures) are similar to those obtained from exponential fits (Table 1). This suggests that kinetic constants of the reaction of reduced P2O with oxygen should be consistent with the values obtained by the simulations (Scheme 1). In the model in Scheme 1, the first step is a bimolecular reaction of the reduced enzyme with oxygen, resulting in formation of a C4a-hydroperoxyflavin intermediate which subsequently decays to yield the oxidized enzyme and H_2O_2. Using this kinetic model, a majority of the absorbance signal detected at the end of the first phase (Figure 2A) should be that of the C4a-hydroperoxyflavin.

Absorbance Characteristics of the Flavin Intermediate. Reaction of reduced P2O with the highest oxygen concentration similar to that in Figure 2 was monitored at 5 nm intervals in the 310−550 nm region using stopped-flow spectrophotometry. Simulations of the reaction of the reduced enzyme and oxygen according to the model in Scheme 1 allow for the determination of the concentration of each species at various stages of the reaction. Therefore, the absorbance of each flavin species can be calculated using the stopped-flow data. Using 23 μM reduced enzyme and 960 μM oxygen, the time when the intermediate was maximally formed (t_{max}) was calculated to be 0.0298 s. At this point, concentrations of E−Fl_{red}, E−Fl−OOH, and E−Fl_{ox} were 4.78, 13.1, and 5.12 μM, respectively. Since the spectra of E−Fl_{red} and E−Fl_{ox} are known, the absorbance of both species according to their concentrations was subtracted from the absorbance of the stopped-flow data. By performing this calculation at various wavelengths in the 310−550 nm region, we obtained a spectrum of E−Fl−OOH (13.1 μM) (the lower black-circle line in Figure 3). A factor of 1.8 was used to multiply this spectrum to increase the absorbance to be equivalent to 23 μM, resulting in a spectrum of the intermediate shown as the higher black-circle line in Figure 3.

The maximum absorbance of the intermediate is observed at 375 nm with no absorption around 450 nm (Figure 3, black-circle line), and the spectral characteristics are very similar to those of flavin C4a-adduct intermediates regularly encountered in flavoprotein monooxygenases (*5, 23*). For the sake of comparison, the spectrum of C4a-hydroperoxyflavin found in the reaction of the monooxygenase component of *p*-hydroxyphenylacetate hydroxylase (C_2) from *Acinetobacter baumannii* (*24, 25*) has been superimposed (Figure 3, dashed line).

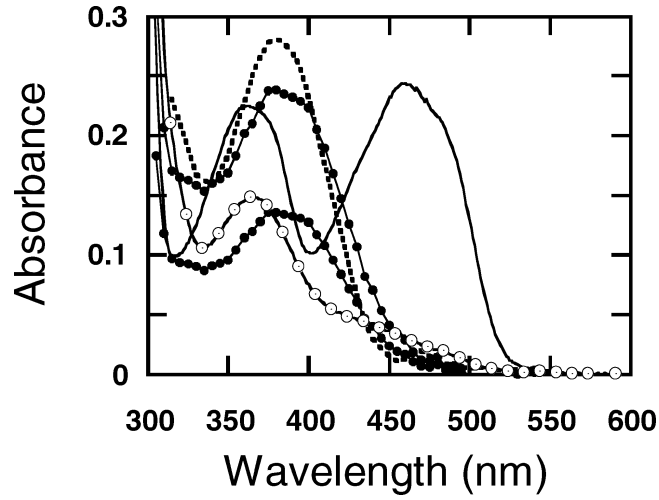

FIGURE 3: Spectra of flavin species, including the intermediate of P2O. An experiment similar to that in Figure 2 was carried out with 0.96 mM oxygen after mixing, and the absorbance was monitored at selected wavelengths between 310 and 550 nm. Data obtained were used to calculate a spectrum of the intermediate. The lower black-circle line represents the spectrum of E−Fl−OOH (13.1 μM) obtained from direct subtraction of the absorbance of E−Fl_{ox} and E−Fl_{red} from the stopped-flow data. The spectrum was multiplied by a factor of 1.8, resulting in the higher black-circle line which represents a spectrum of the intermediate at 23 μM. A spectrum of the reduced enzyme (starting species) is shown as the line with white circles, and that of the fully oxidized enzyme (final species) is shown as the solid line. As a reference, the spectrum of a C4a-hydroperoxyflavin intermediate obtained from a flavoprotein monooxygenase (C_2) (*24*, *25*) is shown as the dashed line.

DISCUSSION

In this work, we show that C4a-hydroperoxyflavin occurs as an intermediate during the oxidative half-reaction of P2O. To the best of our knowledge, this is the first report showing stabilization of a C4a-hydroperoxyflavin under natural turnover conditions by a flavoprotein oxidase. The reaction of reduced P2O with oxygen can be described as in Scheme 1, indicating formation and decay of the intermediate. The spectrum of the C4a-hydroperoxyflavin intermediate reported here (Figure 3) is very similar to the spectra found in the oxidative half-reaction of flavoprotein monooxygases such as aromatic hydroxylases (*26–28*), cyclohexanone monooxygenase (*29*), and bacterial luciferase (*30, 31*). In these enzymes, two types of intermediates, C4a-hydroperoxyflavin or C4a-hydroxyflavin (the intermediate resulting after the oxygenation step), are found to have similar spectral characteristics. Since P2O cannot perform a monooxygenation reaction (*16*) and generates only H_2O_2 during the oxidative half-reaction, the flavin intermediate found in the P2O reaction must be C4a-hydroperoxyflavin.

Until now, only the reaction of P2O reported in this study shows spectroscopic evidence of the formation of C4a-hydroperoxyflavin. The other evidence of the existence of

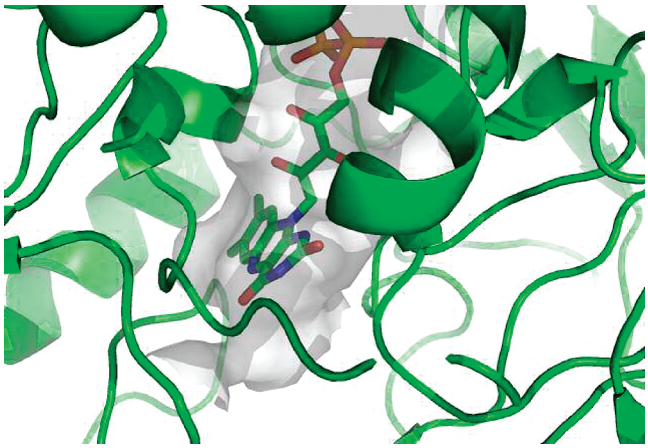

FIGURE 4: Cavity surrounding the FAD molecule in the closed conformation of P2O. In the closed state of P2O (*17*), the active site is completely closed off from the solvent, creating a cavity at the re face of the flavin ring which is rather hydrophobic and provides enough space for accommodation of a peroxide group at the flavin C4a position or any necessary conformational change of the flavin ring that may be needed for formation of the intermediate (C. Divne, personal communication). The gray color represents empty space surrounding the FAD molecule.

the intermediate in flavoprotein oxidase was the detection of a flavin C4a-adduct in the crystalline state of ChO (*14*). Although the FAD C8 M atoms in both P2O and ChO are covalently linked to the proteins via an 8α-(*N*3)-histidyl linkage (*15, 32*), it is unlikely that the stabilization of the flavin C4a-adduct is due to the covalent attachment. In the oxidative half-reaction of AldOx, another oxidase carrying a covalent attachment of the FAD C8 M atom via His, no flavin C4a-adduct was detected (*33*).

It should be noted that, although P2O forms the C4a-hydroperoxyflavin in a manner similar to that of the monooxygenase reaction, the reaction of P2O differs in the sense that the apparent rate constant of the step following formation of the C4a-hydroperoxyflavin is hyperbolically dependent on oxygen concentration (inset of Figure 2B). This behavior is caused by the reversibility of the previous step (Scheme 1, kinetic equations in Experimental Procedures) and is not commonly found in the reactions of flavoprotein monooxygenases (*1, 5*). In monooxygenases, the formation of the C4a-hydroperoxyflavin is usually irreversible, causing the ensuing steps to be independent of oxygen concentration (*25–29*). In flavoprotein oxidases, the reaction of the reduced enzyme with oxygen to form the oxidized enzyme is usually monophasic as in the reaction of *A. niger* GO, in which the flavin oxidation occurs at a forward rate of 2.1×10^6 M^{-1} s^{-1} at 0 °C, and without a reverse rate (*34*). An exception was found in the reaction of cholesterol oxidase (CO) from *Brevibacterium sterolicum* in which the apparent rate for the flavin oxidation was hyperbolically dependent on oxygen concentration (*35*). The result was explained by a model in which the reduced CO exists in two forms and only one form reacts with oxygen (*35*).

Structural Basis of Flavin C4a-Adduct Formation. Only the open form of P2O can accommodate electron donor substrates (*18*) (e.g., monosaccharides during the reductive half-reaction), whereas the closed state has a spatially restricted active site that is fully closed off from the solvent (*17*) (Figure 4). The closed form of P2O has been suggested to represent a conformational state of the active site relevant during the oxidative half-reaction (*17, 18*).

The striking feature of the P2O active site that may facilitate formation of the C4a-hydroperoxyflavin is an elongated, mainly hydrophobic, cavity which is formed at the *re* side of the isoalloxazine ring upon closure of the substrate loop (Figure 4). It was mentioned in the studies of flavin model compounds that stability of the C4a-hydroperoxyflavin was increased in solvents with low dielectric constants (*36*). This cavity also provides enough space to accommodate a peroxide group at the flavin C4a position or any necessary conformational change of the flavin ring that may be needed for formation of the intermediate (C. Divne, personal communication). It has been proposed that one of the key features for stabilization of the C4a-hydroperoxyflavin in flavoprotein monooxygenases is the presence of a cavity and active site residues with optimal geometry to stabilize the intermediate as shown in the structure of the monooxygenase component of *p*-hydroxyphenylacetate hydroxylase (C_2) where such a cavity is present (*12*). In the structure of alditol oxidase (AldOx) where the intermediate is not stabilized, steric hindrance occurred when the C4a-hydroperoxyflavin was modeled into the active site (*13*).

In conclusion, we have shown for the first time the presence of a C4a-hydroperoxyflavin intermediate during the oxidative half-reaction of a flavoprotein oxidase. The P2O intermediate may be a common feature of the oxidative half-reaction of flavoprotein oxidases, but it is conceivable that only certain enzymes are able to sufficiently stabilize the intermediate to allow its identification. This finding should prompt future structural and mechanistic studies of P2O and homologous enzymes aimed at elucidating the crucial factor that enables P2O to stabilize the C4a-hydroperoxyflavin intermediate and what functional advantage P2O has gained from stabilizing this compound. In addition, issues such as what structural factors at the enzyme active site direct the C4a-hydroperoxyflavin to perform nucleophilic/electrophilic monooxygenation or simple H_2O_2 elimination can be addressed in future studies.

ACKNOWLEDGMENT

We thank Drs. Christina Divne, Martin Hallberg, and Andrea Mattevi for useful discussions. We thank Drs. Bruce A. Palfey and Barrie Entsch for critical reading of the manuscript. We are grateful to Dr. Palfey for suggestions about simulations and kinetic analysis. We thank Dr. Poramaet Laowanapiban for assistance in the creation of Figure 4.

REFERENCES

1. Palfey, B. A., and Massey, V. (1998) Flavin-dependent enzymes. In *Comprehensive Biological Catalysis* (Michael, S., Ed.) Vol. 3, pp 83−153, Academic Press, San Diego.
2. Mattevi, A. (2006) To be or not to be an oxidase: Challenging the oxygen reactivity of flavoenzymes. *Trends Biochem. Sci. 31*, 276–283.
3. Fitzpatrick, P. F. (2001) Substrate dehydrogenation by flavoproteins. *Acc. Chem. Res. 34*, 299–307.
4. Bruice, T. C. (1984) Oxygen-flavin chemistry. *Isr. J. Chem. 24*, 54–61.
5. Palfey, B. A., Ballou, D. P., and Massey, V. (1995) Oxygen activation by flavins and pterins. In *Active Oxygen in Biochemistry* (Valentine, J. S., Foote, C. S., Greenberg, A., and Leibman, J. F., Eds.) pp 37−83, Chapman & Hall, Glasgow, U.K.

6. Klinman, J. P. (2001) Life as aerobes: Are there simple rules for activation of dioxygen by enzymes? *J. Biol. Inorg. Chem. 6*, 1–13.
7. Klinman, J. P. (2007) How do enzymes activate oxygen without inactivating themselves? *Acc. Chem. Res. 40*, 325–333.
8. van Berkel, W. J., Kamerbeek, N. M., and Fraaije, M. W. (2006) Flavoprotein monooxygenases, a diverse class of oxidative biocatalysts. *J. Biotechnol. 124*, 670–689.
9. Mallett, T. C., and Claiborne, A. (1998) Oxygen reactivity of an NADH oxidase C42S mutant: Evidence for a C(4a)-peroxyflavin intermediate and a rate-limiting conformational change. *Biochemistry 37*, 8790–8802.
10. Stankovich, M. T., Schopfer, L. M., and Massey, V. (1978) Determination of glucose oxidase oxidation-reduction potentials and the oxygen reactivity of fully reduced and semiquinoid forms. *J. Biol. Chem. 253*, 4971–4979.
11. Ghisla, S., and Massey, V. (1989) Mechanisms of flavoprotein-catalyzed reactions. *Eur. J. Biochem. 181*, 1–17.
12. Alfieri, A., Fersini, F., Ruangchan, N., Prongjit, M., Chaiyen, P., and Mattevi, A. (2007) Structure of the monooxygenase component of a two-component flavoprotein monooxygenase. *Proc. Natl. Acad. Sci. U.S.A. 104*, 1177–1182.
13. Forneris, F., Heuts, D. P., Delvecchio, M., Rovida, S., Fraaije, M. W., and Mattevi, A. (2008) Structural analysis of the catalytic mechanism and stereoselectivity in *Streptomyces coelicolor* alditol oxidase. *Biochemistry 47*, 978–985.
14. Quaye, O., Lountos, G. T., Fan, F., Orville, A. M., and Gadda, G. (2008) Role of Glu312 in binding and positioning of the substrate for the hydride transfer reaction in choline oxidase. *Biochemistry 47*, 243–256.
15. Halada, P., Leitner, C., Sedmera, P., Haltrich, D., and Volc, J. (2003) Identification of the covalent flavin adenine dinucleotide-binding region in pyranose 2-oxidase from *Trametes multicolor*. *Anal. Biochem. 314*, 235–242.
16. Leitner, C., Volc, J., and Haltrich, D. (2001) Purification and characterization of pyranose oxidase from the white rot fungus *Trametes multicolor*. *Appl. Environ. Microbiol. 67*, 3636–3644.
17. Hallberg, B. M., Leitner, C., Haltrich, D., and Divne, C. (2004) Crystal structure of the 270 kDa homotetrameric lignin-degrading enzyme pyranose 2-oxidase. *J. Mol. Biol. 341*, 781–796.
18. Kujawa, M., Ebner, H., Leitner, C., Hallberg, B. M., Prongjit, M., Sucharitakul, J., Ludwig, R., Rudsander, U., Peterbauer, C., Chaiyen, P., Haltrich, D., and Divne, C. (2006) Structural basis for substrate binding and regioselective oxidation of monosaccharides at C3 by pyranose 2-oxidase. *J. Biol. Chem. 281*, 35104–35115.
19. Macheroux, P. (1999) UV-visible spectroscopy as a tool to study flavoproteins. In *Flavoprotein Protocols* (Chapman, S. K., and Reid, G. A., Eds.) pp 1−23, Humana Press, Totowa, NJ.
20. Chaiyen, P., Sucharitakul, J., Svasti, J., Entsch, B., Massey, V., and Ballou, D. P. (2004) Use of 8-substituted-FAD analogues to investigate the hydroxylation mechanism of the flavoprotein 2-methyl-3-hydroxypyridine-5-carboxylic acid oxygenase. *Biochemistry 43*, 3933–3943.
21. Hiromi, K. (1979) Analysis of fast enzyme reactions: Transient kinetics. In *Kinetics of Fast Enzyme Reactions: Theory and Practice*, pp 187−244, Kodansha Ltd., Tokyo.
22. Johnson, K. A. (2003) Transient-state kinetics and computational analysis of transcription initiation. In *Kinetic Analysis of Macromolecules* (Johnson, K. A., and Williams, R., Eds.) pp 87−119, Oxford University Press Inc., New York.
23. Ballou, D., Entsch, B., and Cole, L. J. (2005) Dynamics involved in catalysis by single-component and two-component flavin-dependent aromatic hydroxylases. *Biochem. Biophys. Res. Commun. 338*, 590–598.
24. Sucharitakul, J., Chaiyen, P., Entsch, B., and Ballou, D. P. (2006) Kinetic mechanisms of the oxygenase from a two-component enzyme, *p*-hydroxyphenylacetate 3-hydroxylase from *Acinetobacter baumannii*. *J. Biol. Chem. 281*, 17044–17053.
25. Sucharitakul, J., Phongsak, T., Entsch, B., Svasti, J., Chaiyen, P., and Ballou, D. P. (2007) Kinetics of a two-component *p*-hydroxyphenylacetate hydroxylase explain how reduced flavin is transferred from the reductase to the oxygenase. *Biochemistry 46*, 8611–8623.
26. Entsch, B., Cole, L. J., and Ballou, D. P. (2005) Protein dynamics and electrostatics in the function of *p*-hydroxybenzoate hydroxylase. *Arch. Biochem. Biophys. 433*, 297–311.
27. Chaiyen, P., Brissette, P., Ballou, D. P., and Massey, V. (1997) Unusual mechanism of oxygen atom transfer and product rearrangement in the catalytic reaction of 2-methyl-3-hydroxypyridine-5-carboxylic acid oxygenase. *Biochemistry 36*, 8060–8070.
28. Chaiyen, P., Brissette, P., Ballou, D. P., and Massey, V. (1997) Reaction of 2-methyl-3-hydroxypyridine-5-carboxylic acid (MHPC) oxygenase with N-methyl-5-hydroxynicotinic acid: Studies on the mode of binding, and protonation status of the substrate. *Biochemistry 36*, 13856–13864.
29. Sheng, D., Ballou, D. P., and Massey, V. (2001) Mechanistic studies of cyclohexanone monooxygenase: Chemical properties of intermediates involved in catalysis. *Biochemistry 40*, 11156–11167.
30. Suadee, C., Nijvipakul, S., Svasti, J., Entsch, B., Ballou, D. P., and Chaiyen, P. (2007) Luciferase from *Vibrio campbellii* is more thermostable and binds reduced FMN better than its homologues. *J. Biochem. 142*, 539–552.
31. Macheroux, P., Ghisla, S., and Hastings, J. W. (1993) Spectral detection of an intermediate preceding the excited state in the bacterial luciferase reaction. *Biochemistry 32*, 14183–14186.
32. Fan, F., and Gadda, G. (2007) An internal equilibrium preorganizes the enzyme-substrate complex for hydride tunneling in choline oxidase. *Biochemistry 46*, 6402–6408.
33. Heuts, D. P., van Hellemond, E. W., Janssen, D. B., and Fraaije, M. W. (2007) Discovery, characterization, and kinetic analysis of an alditol oxidase from *Streptomyces coelicolor*. *J. Biol. Chem. 282*, 20283–20291.
34. Gibson, Q. H., Swoboda, B. E., and Massey, V. (1964) Kinetics and mechanism of action of glucose oxidase. *J. Biol. Chem. 239*, 3927–3934.
35. Pollegioni, L., Wels, G., Pilone, M. S., and Ghisla, S. (1999) Kinetic mechanisms of cholesterol oxidase from *Streptomyces hygroscopicus* and *Brevibacterium sterolicum*. *Eur. J. Biochem. 264*, 140–151.
36. Eberlein, G., and Bruice, T. C. (1983) The chemistry of a 1,5-diblocked flavin. 2. Proton and electron transfer steps in the reaction of dihydroflavins with oxygen. *J. Am. Chem. Soc. 105*, 6685–6697.

BI801039D